All-Printed Solid-State Microsupercapacitors Derived from Self-Template Synthesis of Ag@PPy Nanocomposites

Li Liu, Qiang Lu, Shuanglei Yang, Jiang Guo, Qingyong Tian, Weijing Yao, Zhanhu Guo,* Vellaisamy A. L. Roy,* and Wei Wu*

The next-generation energy storage devices are expected to be flexible, cost-effective, and high power storage devices to complement or replace rigid batteries and conventional capacitors for wearable electronic device applications. In this regard, a scalable and cost-effective fabrication of all-printed solid-state microsupercapacitors (MSCs) involving self-template synthesis of Ag@PPy nanocomposites (NCs) as active materials is demonstrated. The as-obtained Ag@PPy NCs exhibit high specific capacitance and are formulated as screen printing inks that are printed to form electrodes on plastic substrates. The Ag current collectors, Ag@PPy NC electrodes, and gel electrolyte are screen printed and fabricated as flexible all-solid-state MSCs exhibiting excellent capacitive features, including remarkable mechanical flexibility of 77.6% after 1000 bending cycles, superior stability of 82.6% after 10000 cycles, and high energy density of 0.00433 mW h cm^{-2}. The Ag@PPy inks are easily prepared and more than 40 printed MSCs are fabricated on flexible plastic substrates in less than 30 min. It is envisioned that the fully printed flexible all-solid-state MSCs could be a promising candidate for flexible energy storage devices.

Dr. L. Liu, Q. Lu, Dr. Q. Y. Tian, Dr. W. J. Yao, Prof. W. Wu
Laboratory of Printable Functional Nanomaterials
and Printed Electronics
School of Printing and Packaging
Wuhan University
Wuhan 430072, P. R. China
E-mail: weiwu@whu.edu.cn
Dr. L. Liu, Q. Lu, Dr. Q. Y. Tian, Dr. W. J. Yao, Prof. W. Wu
Shenzhen Research Institute of Wuhan University
Shenzhen 518057, P. R. China
Dr. S. L. Yang
School of Materials Science and Engineering
Qingdao University
Qingdao 266071, P. R. China
J. Guo, Prof. Z. H. Guo
Integrated Composites Laboratory (ICL)
Chemical and Biomolecular Engineering Department
University of Tennessee
Knoxville, TN 37996, USA
E-mail: zguo10@utk.edu
Prof. V. A. L. Roy
Department of Physics and Materials Science
City University of Hong Kong
Kowloon, Hong Kong SAR 999077, P. R. China
E-mail: val.roy@cityu.edu.hk

1. Introduction

Owing to current development trend toward flexible and portable personal electronics, the emerging field of "printed electronics" has attracted increasing research interests. Considerable efforts have been made to meet the demands for light, flexible, inexpensive, and sustainable electronics.[1–3] The dream of realizing flexible electronics products such as displays, thin-film solar cells, thin-film transistors, and radio frequency identification devices[4–8] can only be possible with flexible, high-power, and stable energy storage devices to power such devices. In this regard, fully flexible microsupercapacitors (MSCs) are essential and show great promise to expedite the dream of flexible electronic devices.

Conventional energy storage devices are mainly limited by their inflexibility, relatively low power density, and long charging time.[9–11] Flexible MSCs are considered as novel energy storage devices with promising features as lightweight, outstanding flexibility, higher power density than batteries, short charging time, and long cycling stability.[12–16] Various methods have been attempted to fabricate flexible MSCs, including chemical vapor deposition,[17] sputtering,[18] and filtration deposition.[19] However, due to their complicated process, limitation of substrates, and expensive cost, the realization of practical MSCs becomes impossible. To overcome these issues, screen printing is a good option for fabricating MSCs on flexible substrates, which is simple, rapid, and inexpensive.[20] Additionally, the screen printing technique allows control over the area and can be printed on various flexible substrates, such as plastics, paper, and cloth.[21,22] Since the inks applied to the process strongly govern the performance of screen-printed flexible MSCs, it is necessary to explore ideal materials for the functional ink formulation. The functional ink should possess versatile properties that can be printed on various substrates with superior electrochemical performance. First and foremost, the ink should be well printable to accommodate the screen printing process. Moreover, the active materials should have high specific capacitance. Finally, the cost should also be taken into account for practical applications.

Polypyrrole-based materials are one of the promising candidates for flexible MSCs, owing to the high pseudocapacitance,

low-cost synthesis, intrinsic flexibility and good environmental stability, easy preparation for large-scale devices, and suitable working window.[23–26] However, it suffers from several disadvantages such as moderate conductivity and poor cycling stability.[27] To overcome these drawbacks, various materials such as carbon,[28] graphene and graphene oxide,[29,30] metallic oxide,[31,32] and metallic particles[33,34] have been incorporated to form composites. Compared with other materials, the metallic (especially silver) particles are widely applied to printed electronics on large-scaled production due to its high conductivity, easy malleability, and low cost.[35] Therefore, the Ag@PPy ink is a great option for fabricating flexible MSCs by the screen printing technique on a large scale. For example, Yuan and co-workers synthesized submicrometer spherical Ag@PPy composites with a moderate specific capacitance of 225.8 F g^{-1} at 1 A g^{-1},[33] which limits their application as practical energy storage devices. Therefore, the Ag@PPy composites with high specific capacitance are essential and need to be developed.

Herein, we develop a simple and rapid method to synthesize Ag@PPy nanocomposites (NCs), and demonstrate their electrochemical performance in a three-electrode electrochemical system. The Ag@PPy NCs with a high specific capacitance (576.6 F g^{-1} at 1 A g^{-1}) are obtained. Furthermore, the functional inks based on Ag@PPy NCs are formulated and show a good printability, low viscosity, and good stability. Moreover, we demonstrate flexible all-solid-state fully printed MSCs on a large scale. Owing to the synergistic effect of Ag@PPy inks and reasonable screen printing process, the flexible and lightweight all-solid-state MSCs exhibit remarkable mechanical flexibility, superior cycling stability (82.6% retention after 10 000 cycles), and high energy density (0.00433 mW h cm^{-2}). The practical use of the all-printed solid-state MSCs is demonstrated by assembling MSC array to light up light-emitting diodes (LEDs), which highlights significant practical applications in flexible electronics.

2. Results and Discussion

2.1. Self-Template Synthesis of Ag@PPy NCs

Ag@PPy NCs were prepared through a simple self-template in situ oxidative polymerization reaction, which is schematically illustrated in **Figure 1**. The synthesis process includes three stages. At stage I, the acid anion groups combine Ag$^+$ to form silv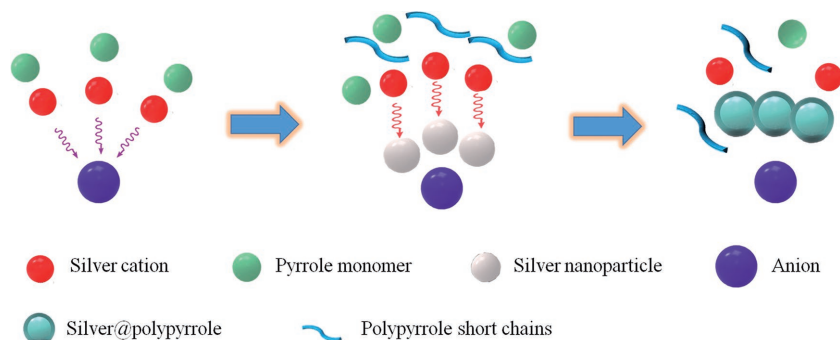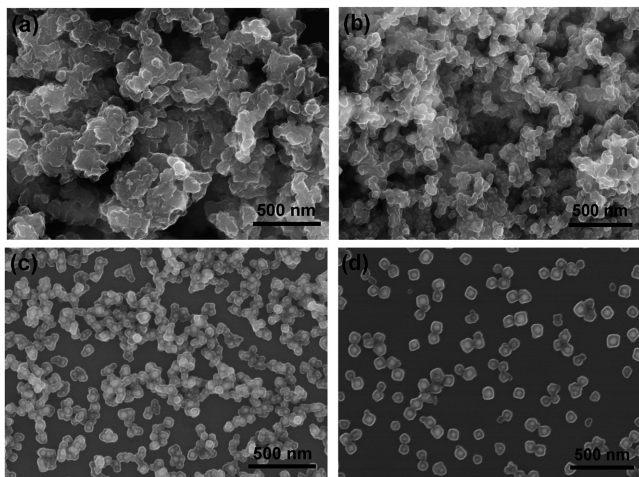er compounds, which act as template (nucleation sites) for in situ oxidative polymerization of Ag$^+$ and pyrrole monomers. The polypyrrole (PPy) short chains are formed together with the formation of silver nanoparticles (NPs) and additional Ag$^+$ are adsorbed onto the surface of Ag NPs because of the conventional ion adsorbed effect (stage II).[36] The surrounding PPy short chains and pyrrole monomers react with Ag$^+$ at the surface of silver NPs (active sites) to form PPy films; eventually, the Ag@PPy NCs are produced (stage III). **Figure 2** presents the scanning electron microscopy (SEM) images of the as-obtained PPy and Ag@PPy NCs. In Figure 2a, the PPy exhibits an agglomeration morphology as reported in the literature.[37] Different Ag@PPy NCs have been synthesized simply by introducing different anions. When the C$_6$H$_5$O$_7^{3-}$ ions are added into the reaction, all Ag NPs are fully coated by PPy films and the as-obtained Ag@PPy NCs present similar morphology as PPy sample (Figure 2b), whereas peasecod-shaped Ag@PPy NCs are synthesized by introducing CH$_3$COO$^-$ ions (Figure 2c). As shown in Figure 2d, the monodispersed spherical Ag@PPy NCs are obtained in the presence of CO$_3^{2-}$ ions and Ag NPs are fully coated by PPy. These results indicate that the formation and growth of the Ag@PPy nuclei have been influenced by anions.

Figure 3a shows the X-ray power diffraction (XRD) patterns of the sample. The broad peak at a 2θ of 20–30° presents a reflection characteristic of PPy, implying the existence of PPy.[38] For the Ag@PPy NCs, all diffraction peaks are identical to pure Ag (JCPDS No. 04-0783), indicating that the Ag^0 is formed in the Ag@PPy NCs.[39] To further confirm the structural features of the products, the Fourier transform infrared (FT-IR) measurements have been carried out (Figure 3b). The peaks at 1561 and 1203 cm^{-1} represent the C=C vibration and C−N stretching vibration of PPy. The peaks at 1043 cm^{-1} are attributed to the =C−H in-plane vibration of PPy, while the peaks at 781 cm^{-1} are due to the C−H out-of-plane deformation vibration of PPy. All these peaks correspond to the results of reported literature.[40] From the above results, it is clear that the PPy is effectively formed by self-template in situ oxidative polymerization reaction. X-ray photoelectron spectroscopy (XPS) has been used to qualitatively examine the Ag@PPy NCs. Figure 3c shows the Ag 3d spectrum of Ag@PPy NCs, including Ag 3d$_{5/2}$ (368.0 eV) and Ag 3d$_{3/2}$ (374.1 eV), further confirming the existence of Ag^0 in Ag@PPy NCs.[41] The N 1s spectrum of Ag@PPy NCs is shown in Figure 3d; the only observed peak at 400.0 eV further demonstrates the existence of PPy.[42]

2.2. Electrochemical Performance of Ag@PPy NCs

To select the Ag@PPy NCs with the highest electrochemical performance for MSC applications, various electrochemical measurements have been carried out. The specific capacitance per mass (C_m) is calculated from the galvanostatic charge–discharge (GCD) curves by the equation of $C_m = I\Delta t/m\Delta V$, where I and Δt are the discharge current and discharge time, respectively, m is the mass loading of active materials within the

Figure 1. Schematic illustration of the self-template formation mechanism of Ag@PPy NCs.

Silver cation

Pyrrole monomer

Silver nanoparticle

Anion

Silver@polypyrrole

Polypyrrole short chains

**ADVANCED
SCIENCE NEWS**
www.advancedsciencenews.com

**ADVANCED
MATERIALS
TECHNOLOGIES**
www.advmattechnol.de

Figure 2. SEM images of a) PPy, b) Ag@PPy-1, c) Ag@PPy-2, and d) Ag@PPy-3.

electrode, and ΔV is the operating potential window. The cyclic voltammetry (CV) plots of all sample electrodes with a scan rate of 10 mV s^{-1} are performed and shown in **Figure 4**a; the redox peaks of Ag$^+$/Ag occur at 0.24 and 0.42 V, implying the presence of Ag^0.[43] The Ag@PPy NC electrode exhibits a larger area in the CV curves than PPy electrode, resulting in an enhancement of the capacitance, and Ag@PPy-2 electrode reveals the largest area of CV curves, indicating that Ag@PPy-2 has the highest capacitance. The charge/discharge behavior of all sample electrodes was further demonstrated at a current density of 1 A g^{-1}
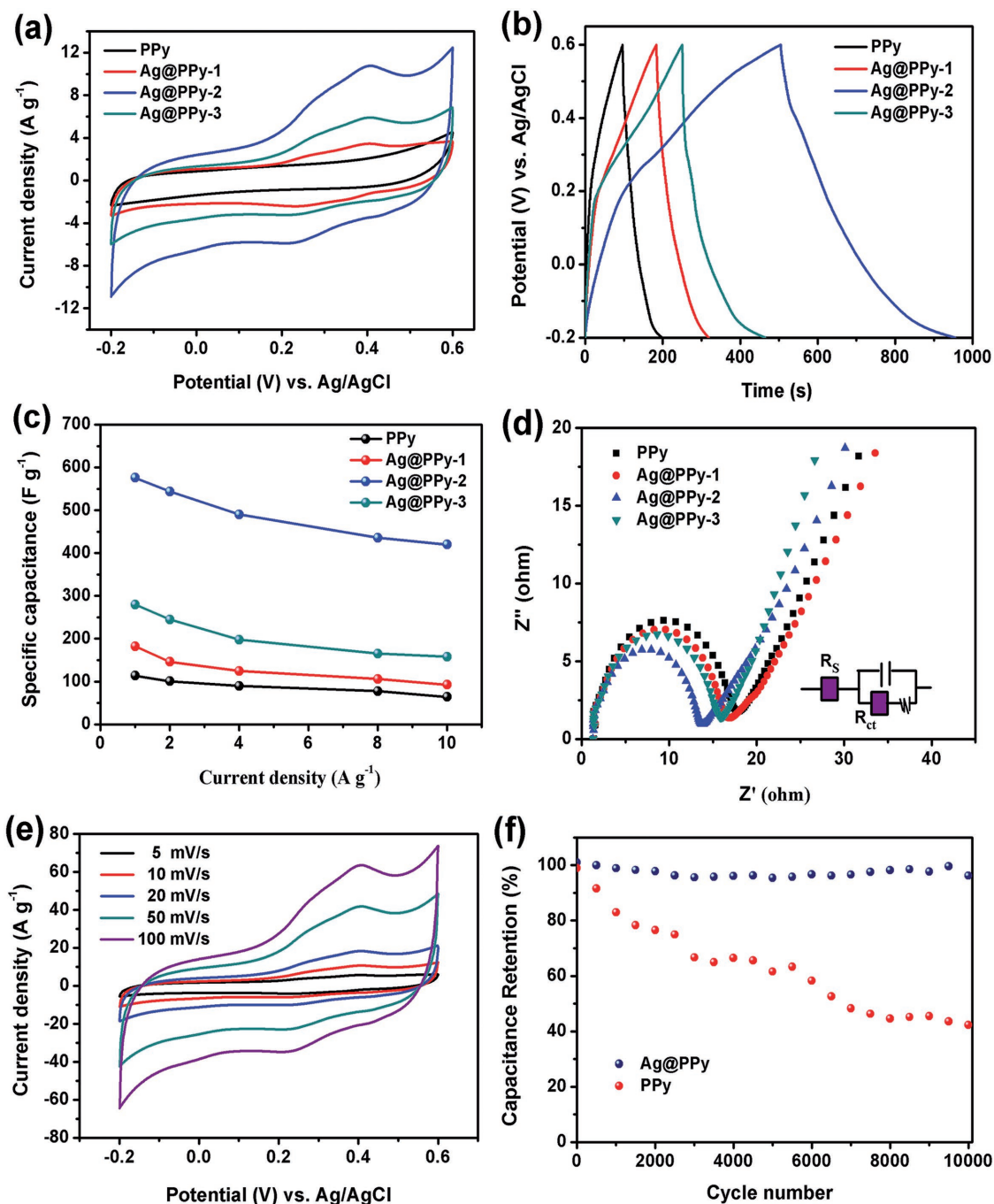
(Figure 4b); all GCD curves are almost symmetrical, suggesting a good capacitive behavior. The Ag NP and PPy functionalization greatly enhances the specific capacitance, increasing from 113.8 F g^{-1} of PPy to 576.6 F g^{-1} of Ag@PPy-2.

Figure 4c shows the specific capacitances of all sample electrodes at different current densities, which are calculated from the discharge curves (Figure S2, Supporting Information). It can be observed that the Ag@PPy-2 electrode shows the highest specific capacitance at all current densities; it is almost 400% increment compared with the PPy electrode. Additionally, the specific capacitance of the Ag@PPy-2 at 10 A g^{-1} remains as high as 420 F g^{-1}, indicating that the Ag@PPy-2 electrode can operate at relatively high current densities. Figure 4d shows the Nyquist plots of all sample electrodes, which are recorded by the electrochemical impedance spectroscopy (the inset is the equivalent circuit illustration). A typical semicircle electrochemical capacitor behavior is observed in all Nyquist plots, which is related to the charge transfer resistance (R_{ct}) and equivalent resistance (R_c). The PPy electrode shows the largest semicircle, while the Ag@PPy-2 electrode shows the smallest semicircle. This result indicates that the Ag@PPy-2 electrode has the lowest R_{ct} compared with other sample electrodes, which is beneficial to capacitance behavior. Therefore, we select the Ag@PPy-2 to formulate the Ag@PPy inks for fabricating MSCs.

In order to further demonstrate the capacitance behavior of Ag@PPy-2, CV analysis at different scan rates (from 5 to 100 mV s^{-1}) has been carried out. As shown in Figure 4e, all CV curves exhibit almost the same shape, revealing excellent capacitance behavior of Ag@PPy-2. Figure 4f shows the long
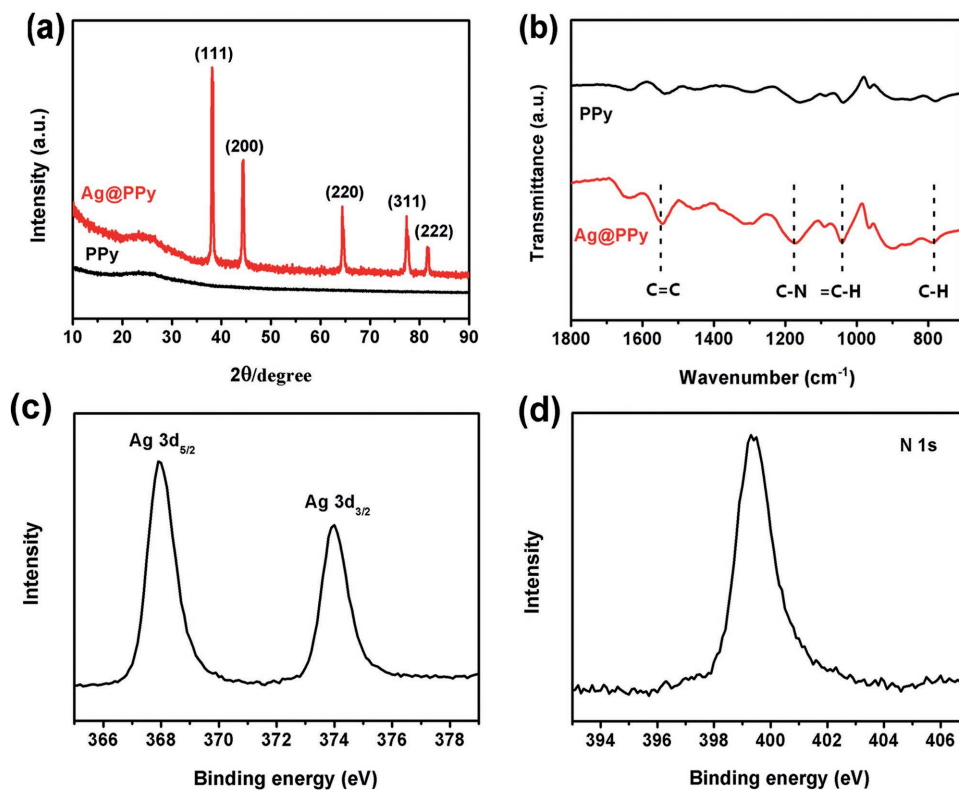
Figure 3. a) XRD patterns, b) FT-IR spectra of PPy and Ag@PPy NCs, c) XPS results of Ag 3d, and d) N 1s of the Ag@ppy NCs.

**ADVANCED
SCIENCE NEWS**

www.advancedsciencenews.com

**ADVANCED
MATERIALS
TECHNOLOGIES**

www.advmattechnol.de

Figure 4. a) CV curves at a scan rate of 10 mV s^{-1}, b) GCD curves measured with a current density of 1 A g^{-1}, c) capacitance retention versus current density, and d) Nyquist plots of various Ag@PPy NCs electrodes and PPy electrode. e) CV curves of Ag@PPy-2 electrode at different scan rates. f) Cyclic stability of PPy and Ag@PPy-2 at 20 A g^{-1} for 10 000 cycles.

cycle life measurements of PPy and Ag@PPy-2. The cycling stability of pure PPy is greatly improved by the addition of Ag NPs; similar results have been reported in the silica and graphite oxide polyaniline system.[44,45] The Ag@PPy-2 exhibits superior cycling stability, i.e., 96.2% of specific capacitance even after 10 000 cycles, but the PPy just retains 41.6% of specific capacitance after 10 000 cycles.

2.3. Electrochemical Performance of the Ag@PPy NC Flexible All-Solid-State MSCs

The flexible MSCs are fabricated by screen printing of Ag@PPy inks onto polyethylene terephthalate (PET) substrates. The screen printing technique is cost effective and easily scalable. In our work, 40 MSCs can be produced on a PET substrate in
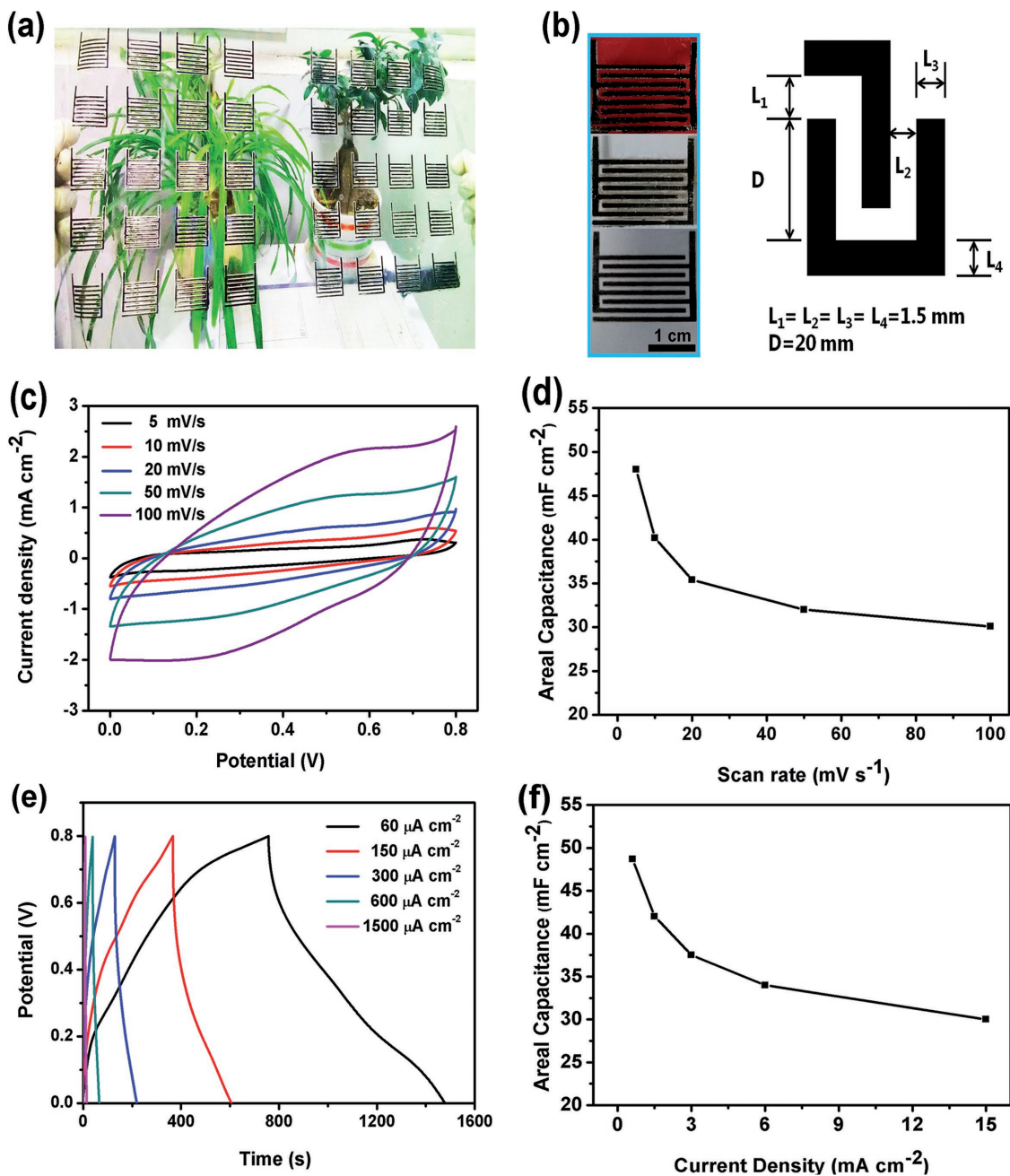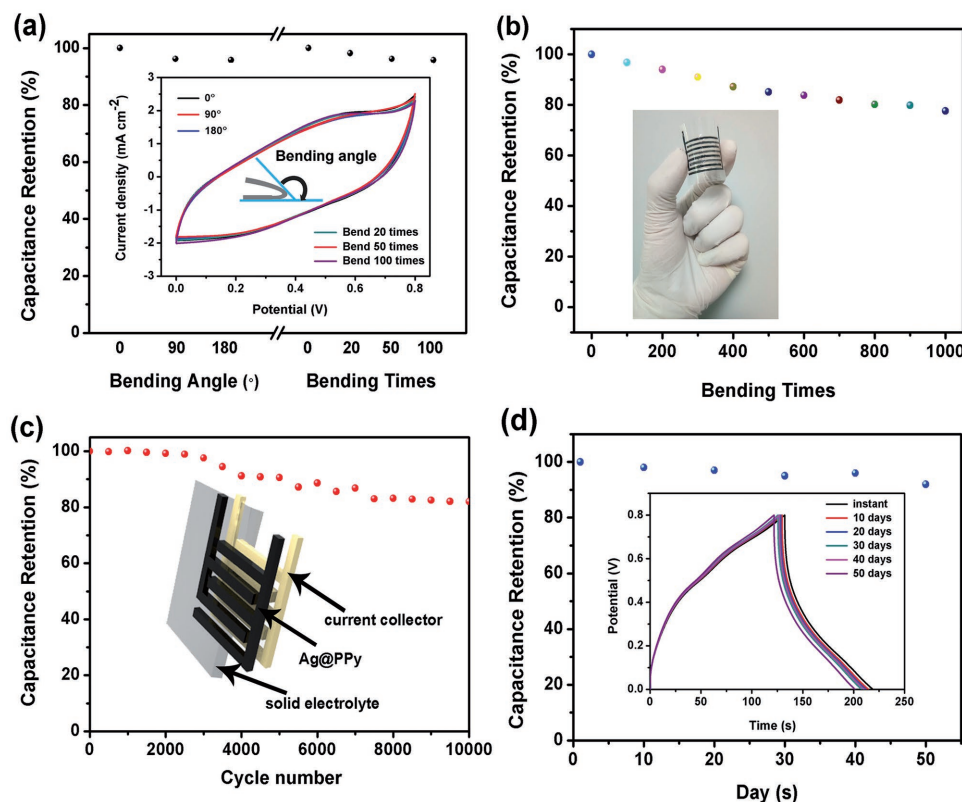
Figure 5. a) Optical photographs scalable fabrication of MSC arrays on the PET substrates. b) Optical photographs of fabricated MSCs on various substrates: cloth, PET, and paper. c) CV and d) scan rate ability of the fabricated MSCs. e) GCD curves and f) current density ability of the MSCs.

just 30 min (**Figure 5**a). Various substrates are demonstrated to fabricate MSCs and the size of MSCs is illustrated (Figure 5b). The thickness and surface morphology of the interdigital electrodes are tested by SEM, which are shown in Figure S3 in the Supporting Information. Figure 5c shows the CV plots of the MSCs at different scan rates (from 5 to 100 mV s⁻¹), and almost rectangular shapes are observed; the corresponding scan rate ability and areal capacitance are shown in Figure 5d. The GCD curves with good linear profiles at various current densities (0.2–5 A g⁻¹) are shown in Figure 5e. The areal specific capacitances based on GCD curves are calculated and

shown in Figure 5f; the maximum areal specific capacitance is 47.5 mF cm⁻² at 60 µA cm⁻². These results confirm an ideal capacitance of the MSCs.

The excellent mechanical robustness of the flexible MSCs is further confirmed by the bending test. **Figure 6**a shows the influence of bending angles (90° and 180°) and bending times (20, 50, and 100 times) on the capacitance retention. The CV curves at different bending conditions show nearly the same shape, indicating that the electrochemical property of flexible MSCs is almost unvaried under different bending angles and bending times. In terms of flexibility the fabricated MSCs

**ADVANCED
SCIENCE NEWS**
www.advancedsciencenews.com

**ADVANCED
MATERIALS
TECHNOLOGIES**
www.advmattechnol.de

Figure 6. a) Capacitance retention ratio of the MSCs at 100 mV s^{-1} for different angles and number of bending times. b) Specific capacitance versus bending times of the fabricated MSCs. c) Cycling behavior of the MSC at 30 mA cm^{-2}. d) Capacitance retention ratio of the MSCs at 300 μA cm^{-2} for different time durations.

possess excellent flexibility of 77.6% after 1000 bending times (Figure 6b). The cycling behavior of the fabricated MSCs is detected by a cyclic charge/discharge process under the bending condition at a fixed current density of 30 mA cm^{-2} (Figure 6c). The fabricated MSCs still maintain 82.6% of specific capacitance after 10 000 cycles, demonstrating its long-term cycling stability. This can be ascribed to the stable structure of the Ag@PPy NCs and electrode formation process of the screen printing. The Ag NPs existing in the Ag@PPy NCs act as an efficient scaffold to support the brittle and weak PPy materials and keep an integrated structure during the process of fast cyclic charge/discharge process. Additionally, the Ag@PPy electrodes and silver current collectors obtained by full screen printing process keep a good connection with each other for mechanical stability and structural integrity during the cyclic charge/discharge process, which is beneficial to improve the cycling stability of the MSC. The stability of fabricated MSCs is also investigated; 92.3% of specific capacitance is remained after 50 d in ambient condition (Figure 6d). These results demonstrate the great potential of our fully printed flexible all-solid-state MSCs for flexible high-power and portable energy storage systems, and also the screen printing technique that has been used is a rapid, low-cost, and practical approach to fabricate MSCs.

In practical applications, the energy that a single MSC can store is too low to meet the required voltage and capacitance of devices. Hence, an array of MSCs is necessary for power supply. To demonstrate the potential practical applications of flexible all-solid-state MSCs, we have connected three MSCs in series and in parallel to make a tandem and multipled device. Each MSC used here has almost the same mass loading of Ag@PPy NCs. The tandem and multipled device is tested by CV and GCD measurements (Figure S4, Supporting Information). As shown in **Figure 7**a, the potential window is enlarged from 0.8 V (a single MSC) to 2.4 V (tandem device). Moreover, the discharge time of the multipled device is tripled that of a single MSC (Figure 7b). These results indicate that the flexible all-solid-state MSCs can be assembled to afford operating voltage and capacitance for practical applications. The energy and power densities are calculated from GCD curves according to $E_{cell} = (C\Delta V^2)/2$ and $P_{cell} = E_{cell}/\Delta t$, respectively, where C is the areal specific capacitance, ΔV is the potential window, Δt is the discharge time, E_{cell} is the energy density, and P_{cell} is the power density. Figure 7c shows the Ragone plots of the flexible all-solid-state MSC. It can be observed that various power densities can be reached with various energy densities. The maximum energy density is 0.00433 mW h cm^{-2} at a power density of 0.02597 mW cm^{-2}, and the highest power density is 0.6 mW cm^{-2} at an energy density of 0.00267 mW h cm^{-2} under an operating voltage window of 0.8 V, which are comparable to previously reported MSCs.[46–51] These results show the successful demonstration of screen printing process and corresponding ink formulation based on Ag@PPy NCs with a high specific capacitance. As shown in Figure 7d and Video S1 (Supporting
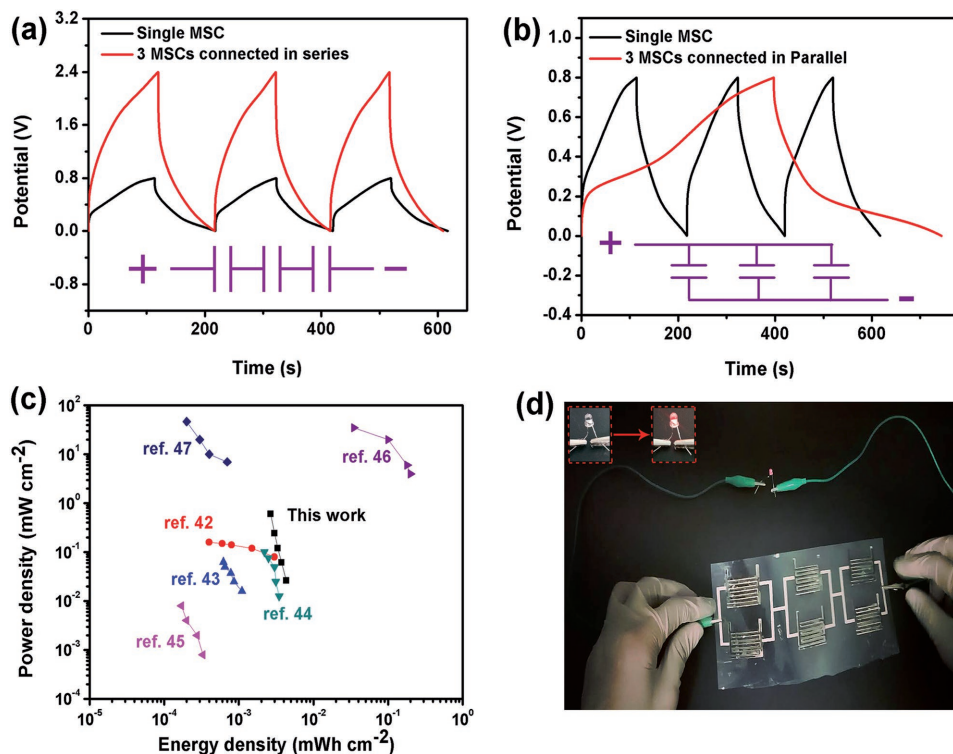
Figure 7. GCD curves for three MSCs connected a) in series and b) in parallel. A single MSC is shown for comparison. The insets are circuit illustrations of the MSCs. c) Ragone plots of the fabricated MSC comparing with previously reported MSCs in other literatures. d) Optical image of a red LED powered by six charged MSCs connected in a combination of series and parallel; the inset shows the digital pictures of initial extinct LED and alight LED powered by MSCs.

Information), a red color LED (1.9 V) could be readily powered up by an array of six charged MSCs, further highlighting the potential practical applications of the fabricated flexible fully printed all-solid-state MSCs as future flexible and portable power supply.

3. Conclusion

A facile and scale-up self-template method to synthesize Ag@PPy NCs with high electrochemical performance is reported and optimal Ag@PPy inks have been successfully used for screen printing electrodes for MSCs. A flexible all-printed solid-state MSC with an extremely high energy density (0.00433 mW h cm^{-2}), remarkable flexibility (77.6% remained after 1000 bending times), and cyclic stability (82.6% remained after 10 000 cycles) has been obtained by a simple screen printing technique. The fabricated MSCs are assembled for practical applications in a large scale. We envision that the screen printed flexible all-solid-state MSCs can be a promising flexible energy storage system for high-performance flexible and portable energy storage in the future.

4. Experimental Section

Materials and Chemicals: Pyrrole (C_4H_5N, GR) and silver nitrate ($AgNO_3$, 99%) were purchased from Aladdin Chemistry Co., Ltd.

Trisodium citrate dehydrate ($C_6H_5Na_3O_7 \cdot 2H_2O$, 99%), sodium acetate ($CH_3COONa$, AR), sodium carbonate (Na_2CO_3, AR), iron(III) chloride hexahydrate ($FeCl_3 \cdot 6H_2O$, GR), poly(*N*-vinylpyrrolidone) (PVP, GR), and polyvinyl alcohol (PVA) were purchased from Sinopharm Chemical Reagent Co., Ltd. Silver conductive paste was purchased from KunShan Hisense Electronics Co., Ltd. Acetylene black was purchased from Taiyuan Lizhiyuan Battery Co., Ltd. Waterborne resin was purchased from Chengdu Indigo Power Sources Co., Ltd. PET was used as the flexible substrate. Deionized water (DI, 18.2 MΩ) was used during the experiment.

Synthesis of Ag@PPy NCs and Formulation of Inks: The Ag@PPy NCs were synthesized from silver nitrate and pyrrole via self-template in situ oxidative polymerization reaction. Different Ag@PPy NCs were obtained by introducing $C_5H_7O_5COO^-$, CH_3COO^-, and CO_3^{2-} and assigned as Ag@ppy-1, Ag@ppy-2, and Ag@ppy-3, respectively. In a typical process, 0.0425 g $AgNO_3$, 0.1 g PVP, and 0.0205 g CH_3COONa were consecutively dissolved in 10 mL DI water under stirring for 10 min, and 10 mL 0.025 M pyrrole monomer aqueous solution was added drop wise with stirring. Afterward, 10 mL 0.03 M $FeCl_3 \cdot 6H_2O$ aqueous solution was added drop wise to accelerate the reaction. After reaction at room temperature for 2 h, the Ag@ppy NCs were obtained and successively washed several times with ethanol and DI water. Pure PPy was also prepared with the same procedures without silver nitrate for comparison. Subsequently, the as-prepared PPy and Ag@PPy NCs were dried at 70 °C in a vacuum oven for 12 h before formulating inks. The Ag@ppy inks were formulated by redispersing 65 wt% as-synthesized Ag@ppy NCs, 15 wt% conductive carbon black, and 20 wt% waterborne resin into DI water. The PPy inks were prepared with the same procedures for comparison.

Fabrication of Flexible All-Solid-State MSCs: The process of fabricating MSCs is illustrated in **Scheme 1**. The interdigital silver current collectors were formed on a PET substrate through a screen printing method
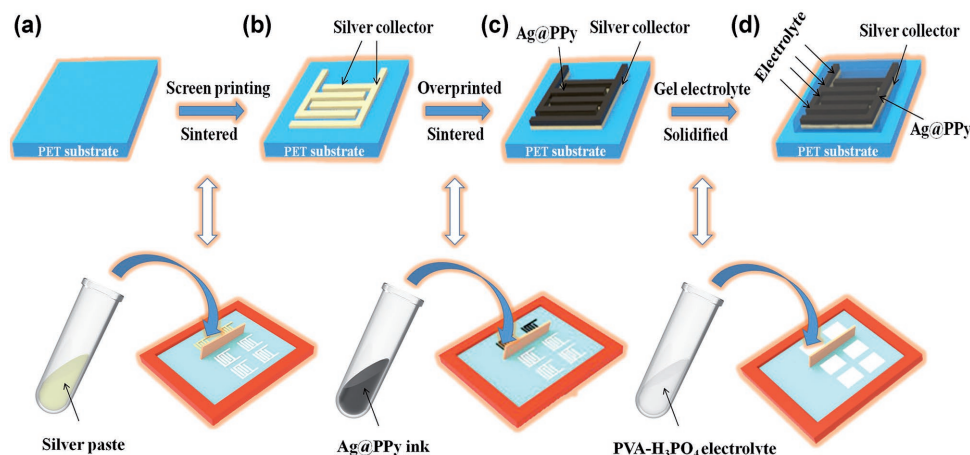
Scheme 1. Scheme illustrating the fabrication process of a flexible all-solid-state MSC. a) The Ag current collector is screen printed on a flexible substrate. b) The Ag@PPy ink is overprinted on top of the silver current collector. Gel electrolyte is then c) screen printed on the top of the device and d) solidified in ambient conditions.

(a), followed by sintering in a vacuum oven at 120 °C. Subsequently, the Ag@PPy inks were overprinted onto the surface of silver current collector (b) and then dried in a vacuum oven at 50 °C. The gel electrolyte (PVA-H_3PO_4) was prepared via adding 10 g H_3PO_4 and 10 g PVA into 100 mL DI water, and heated to 85 °C under stirring for 3 h. Then, the gel electrolyte was fully printed on the top of the device (c) and dried in ambient conditions (d). The details of screen printing process are schematically illustrated in Figure S1 in the Supporting Information.

Characterization: SEM images were recorded on field emission SEM (Hitachi, S-4800). The XRD patterns were recorded using a diffractometer (X' Pert Pro, PANalytical) equipped with a Cu Kα radiation source ($\lambda = 1.5406$ Å). FT-IR spectrum was taken on Nicolet 5700. XPS spectra were performed on Thermo Fisher Scientific ESCALAB 250 Xi system using an Al-Kα radiation source.

Electrochemical Tests: All the electrochemical measurements were recorded with a CHI 660E electrochemical workstation and a CT2001A blue electric battery test system. The electrochemical performance of sample materials was tested via a three-electrode electrochemical system in 0.1 M Na_2SO_4. A platinum wire and Ag/AgCl electrode were used as counter and reference electrodes, respectively. The electrochemical performance of MSCs was measured in a two-electrode system with the prepared gel electrolyte.

Supporting Information

Supporting Information is available from the Wiley Online Library or from the author.

Conflict of Interest

The authors declare no conflict of interest.

[1] L. Li, Z. Wu, S. Yuan, X.-B. Zhang, *Energy Environ. Sci.* **2014**, *7*, 2101.
[2] X. Chen, *Small Methods* **2017**, *1*, 1600029.
[3] K. Sun, P. Xie, Z. Wang, T. Su, Q. Shao, J. Ryu, X. Zhang, J. Guo, A. Shankar, J. Li, R. Fan, D. Cao, Z. Guo, *Polymer* **2017**, *125*, 50.
[4] X. Cao, C. Lau, Y. Liu, F. Wu, H. Gui, Q. Liu, Y. Ma, H. Wan, M. R. Amer, C. Zhou, *ACS Nano* **2016**, *10*, 9816.
[5] C. M. Homenick, R. James, G. P. Lopinski, J. Dunford, J. Sun, H. Park, Y. Jung, G. Cho, P. R. Malenfant, *ACS Appl. Mater. Interfaces* **2016**, *8*, 27900.
[6] X. Gu, Y. Zhou, K. Gu, T. Kurosawa, Y. Guo, Y. Li, H. Lin, B. C. Schroeder, H. Yan, F. Molina-Lopez, *Adv. Energy Mater.* **2017**, *7*, 1602742.
[7] J. Li, L. Xu, C. W. Tang, A. A. Shestopalov, *ACS Appl. Mater. Interfaces* **2016**, *8*, 16809.
[8] T. Liu, K. Yu, L. Gao, H. Chen, N. Wang, L. Hao, T. Li, H. He, Z. Guo, *J. Mater. Chem. A* **2017**, *5*, 17848.
[9] P. G. Bruce, S. A. Freunberger, L. J. Hardwick, J.-M. Tarascon, *Nat. Mater.* **2012**, *11*, 19.
[10] M. F. El-Kady, R. B. Kaner, *Nat. Commun.* **2013**, *4*, 1475.
[11] D. Qi, Y. Liu, Z. Liu, L. Zhang, X. Chen, *Adv. Mater.* **2017**, *29*, 1602802.
[12] H. Hu, Z. Pei, H. Fan, C. Ye, *Small* **2016**, *12*, 3059.
[13] W. Si, C. Yan, Y. Chen, S. Oswald, L. Han, O. G. Schmidt, *Energy Environ. Sci.* **2013**, *6*, 3218.
[14] A. Liu, P. Kovacik, N. Peard, W. Tian, H. Goktas, J. Lau, B. Dunn, K. K. Gleason, *Adv. Mater.* **2017**, *29*, 1606091
[15] A. Ramadoss, K.-Y. Yoon, M.-J. Kwak, S.-I. Kim, S.-T. Ryu, J.-H. Jang, *J. Power Sources* **2017**, *337*, 159.
[16] C. S. Luo, P. Wan, H. Yang, S. A. A. Shah, X. Chen, *Adv. Funct. Mater.* **2017**, *27*, 1606339.
[17] X. Wang, G. Yushin, *Energy Environ. Sci.* **2015**, *8*, 1889.

**ADVANCED
SCIENCE NEWS**

www.advancedsciencenews.com

**ADVANCED
MATERIALS
TECHNOLOGIES**

www.advmattechnol.de

[18] M. Létiche, K. Brousse, A. Demortière, P. Huang, B. Daffos, S. Pinaud, M. Respaud, B. Chaudret, P. Roussel, L. Buchaillot, *Adv. Funct. Mater.* **2017**, *27*, 1606813.

[19] Y. Yu, J. Zhong, W. Sun, R. Kumar, N. Koratkar, *Adv. Funct. Mater.* **2017**, *28*, 1606461.

[20] Z. Tehrani, D. Thomas, T. Korochkina, C. Phillips, D. Lupo, S. Lehtimäki, J. O'Mahony, D. Gethin, *Energy* **2017**, *118*, 1313.

[21] Y. D. Kim, J. Hone, *Nature* **2017**, *544*, 167.

[22] W. Wu, *Nanoscale* **2017**, *9*, 7342.

[23] Y. Huang, H. Li, Z. Wang, M. Zhu, Z. Pei, Q. Xue, Y. Huang, C. Zhi, *Nano Energy* **2016**, *22*, 422.

[24] A. Afzal, F. A. Abuilaiwi, A. Habib, M. Awais, S. B. Waje, M. A. Atieh, *J. Power Sources* **2017**, *352*, 174.

[25] J. Guo, H. Song, H. Liu, C. Luo, Y. Ren, T. Ding, M. A. Khan, D. P. Young, X. Liu, X. Zhang, J. Kong, Z. Guo, *J. Mater. Chem. C* **2017**, *5*, 5334.

[26] C. Yang, H. Wei, L. Guan, J. Guo, Y. Wang, X. Yan, X. Zhang, S. Wei, Z. Guo, *J. Mater. Chem. A* **2015**, *3*, 14929.

[27] H. Kashani, L. Chen, Y. Ito, J. Han, A. Hirata, M. Chen, *Nano Energy* **2016**, *19*, 391.

[28] X. Li, I. Zhitomirsky, *J. Power Sources* **2013**, *221*, 49.

[29] Y. Zhao, J. Liu, Y. Hu, H. Cheng, C. Hu, C. Jiang, L. Jiang, A. Cao, L. Qu, *Adv. Mater.* **2013**, *25*, 591.

[30] H.-H. Chang, C.-K. Chang, Y.-C. Tsai, C.-S. Liao, *Carbon* **2012**, *50*, 2331.

[31] Y. Chen, B. Liu, Q. Liu, J. Wang, Z. Li, X. Jing, L. Liu, *Nanoscale* **2015**, *7*, 15159.

[32] J. Hu, M. Li, F. Lv, M. Yang, P. Tao, Y. Tang, H. Liu, Z. Lu, *J. Power Sources* **2015**, *294*, 120.

[33] L. Yuan, C. Wan, X. Ye, F. Wu, *Electrochim. Acta* **2016**, *213*, 115.

[34] H. Moon, H. Lee, J. Kwon, Y. D. Suh, D. K. Kim, I. Ha, J. Yeo, S. Hong, S. H. Ko, *Sci. Rep.* **2017**, *7*, 41981.

[35] W. Shen, X. Zhang, Q. Huang, Q. Xu, W. Song, *Nanoscale* **2014**, *6*, 1622.

[36] M. Chang, T. Kim, H. W. Park, M. Kang, E. Reichmanis, H. Yoon, *ACS Appl. Mater. Interfaces* **2012**, *4*, 4357.

[37] P. Pattananuwat, D. Aht-ong, *Electrochim. Acta* **2017**, *224*, 149.

[38] Z. W. Seh, H. Wang, P.-C. Hsu, Q. Zhang, W. Li, G. Zheng, H. Yao, Y. Cui, *Energy Environ. Sci.* **2014**, *7*, 672.

[39] C. Wang, B. Cheng, H. Zhang, P. Wan, L. Luo, Y. Kuang, X. Sun, *Nano Res.* **2016**, *9*, 1532.

[40] X. Sun, H. Zhang, L. Zhou, X. Huang, C. Yu, *Small* **2016**, *12*, 3732.

[41] S.-F. Yang, C.-G. Niu, D. Huang, H. Zhang, C. Liang, G. Zeng, *Environ. Sci.: Nano* **2017**, *4*, 585.

[42] C. Yu, P. Ma, X. Zhou, A. Wang, T. Qian, S. Wu, Q. Chen, *ACS Appl. Mater. Interfaces* **2014**, *6*, 17937.

[43] A. Safavi, R. Ahmadi, Z. Mohammadpour, *Sen. Actuators, B* **2017**, *242*, 609.

[44] H. Wei, H. Gu, J. Guo, S. Wei, J. Liu, Z. Guo, *J. Phys. Chem. C* **2013**, *117*, 13000.

[45] H. Wei, J. Zhu, S. Wu, S. Wei, Z. Guo, *Polymer* **2013**, *54*, 1820.

[46] L. Li, Z. Lou, W. Han, D. Chen, K. Jiang, G. Shen, *Adv. Mater. Technol.* **2017**, *2*, 1600282.

[47] M. Zhu, Y. Huang, Y. Huang, H. Li, Z. Wang, Z. Pei, Q. Xue, H. Geng, C. Zhi, *Adv. Mater.* **2017**, *29*, 1605137.

[48] M. Wu, Y. Li, B. Yao, J. Chen, C. Li, G. Shi, *J. Mater. Chem. A* **2016**, *4*, 16213.

[49] Y. Wang, Y. Shi, C. X. Zhao, J. I. Wong, X. W. Sun, H. Y. Yang, *Nanotechnology* **2014**, *25*, 094010.

[50] Q. Jiang, N. Kurra, C. Xia, H. N. Alshareef, *Adv. Energy Mater.* **2016**, *7*, 1601257.

[51] N. Kurra, B. Ahmed, Y. Gogotsi, H. N. Alshareef, *Adv. Energy Mater.* **2016**, *6*, 1601372.